Improvements in silicon solar cells efficiency with Photonic crystals

Vittorio Di Trapani, Ph.D. candidate University of Siena

Outline

- Introduction
- Limiting factors to conversion efficiency
- Solutions to cope with common limiting factors
- Photonic crystals: a brief introduction
- Photonic crystals in solar cells
    - Wave-interference based light-trapping in photonic crystals
    - Other applications

Introduction

Energy production

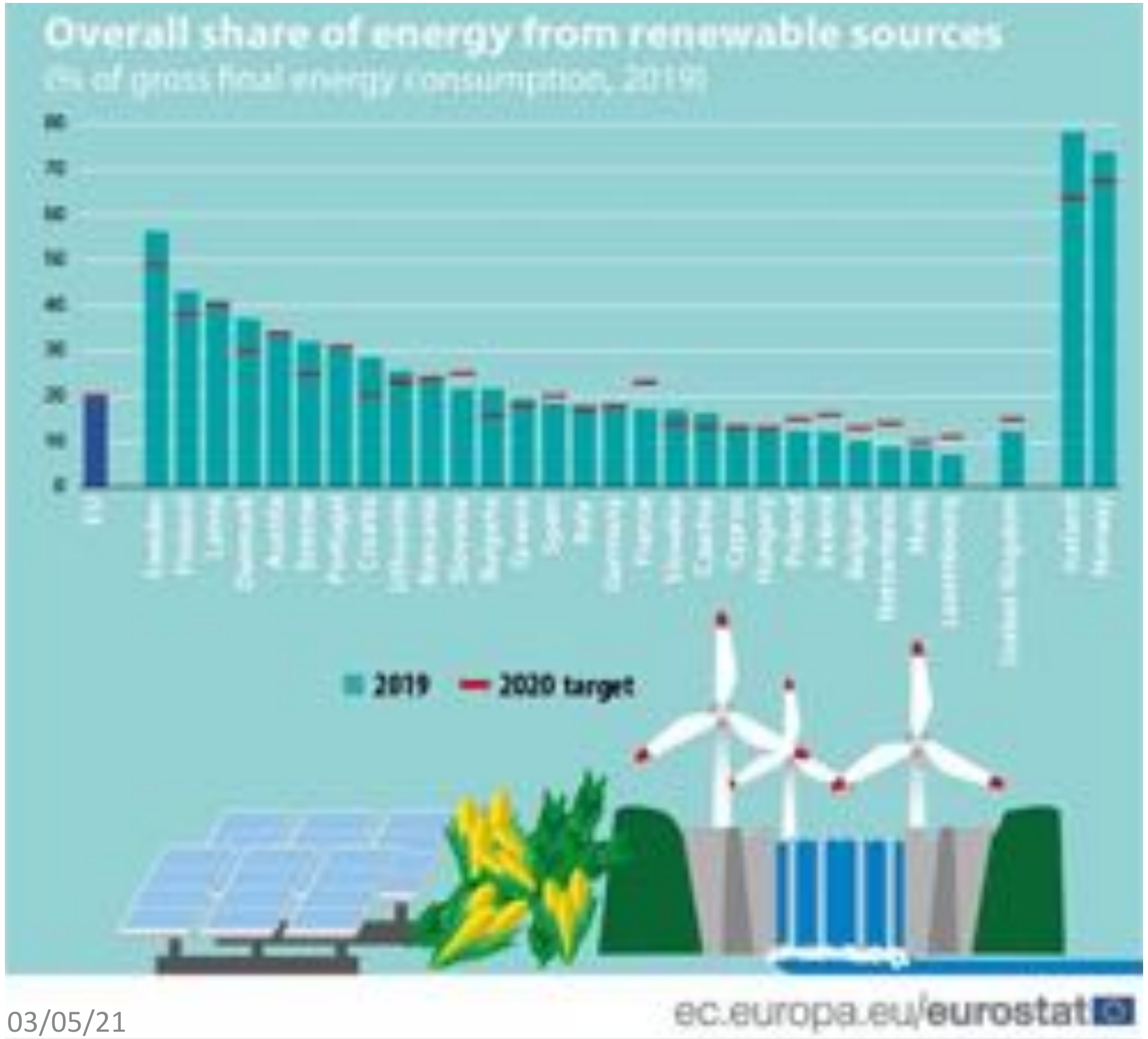

Solar spectrum

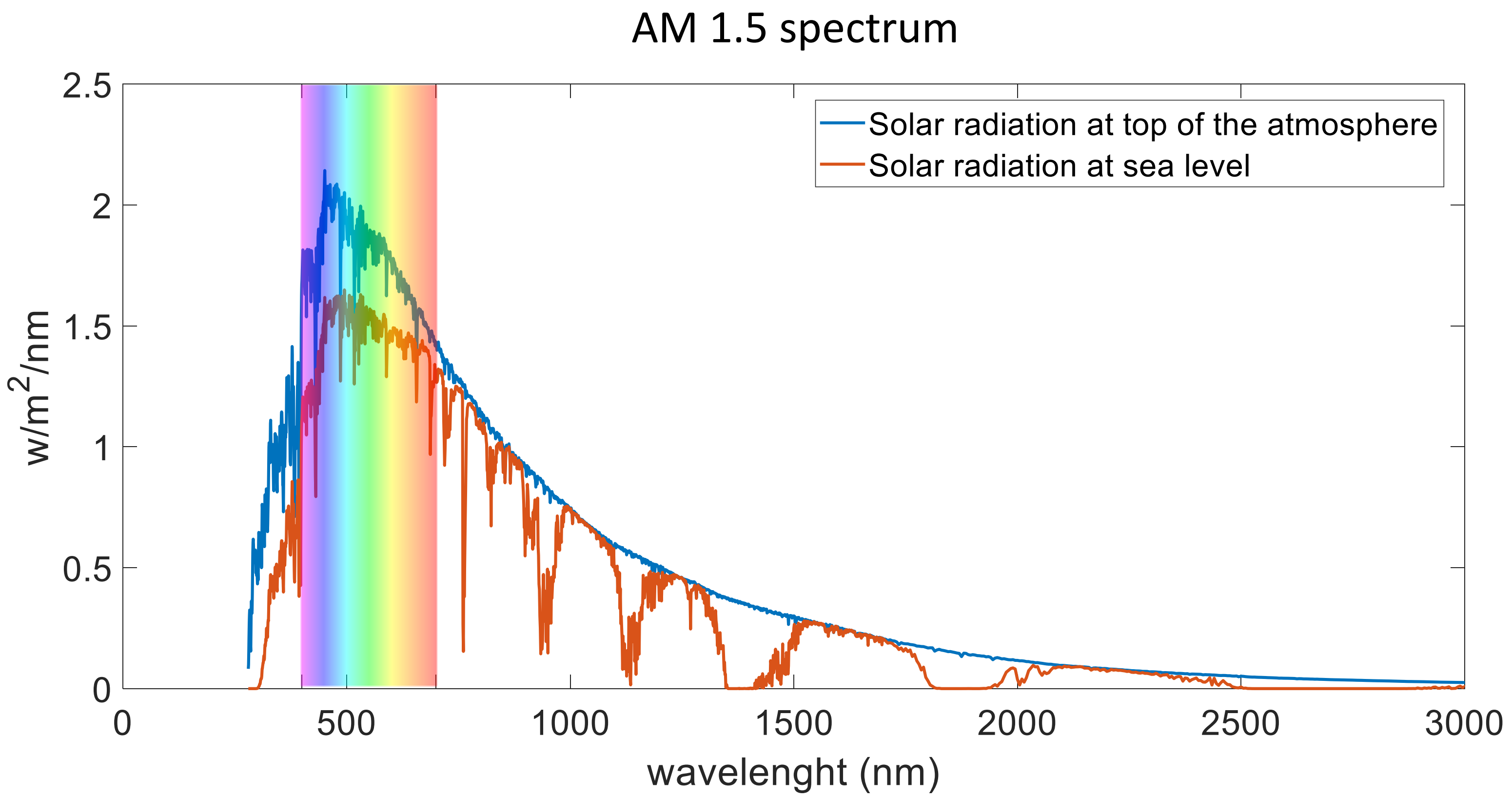
AM 1.5 spectrum

Data from https://www.nrel.gov/grid/solar-resource/spectra-am1.5.html

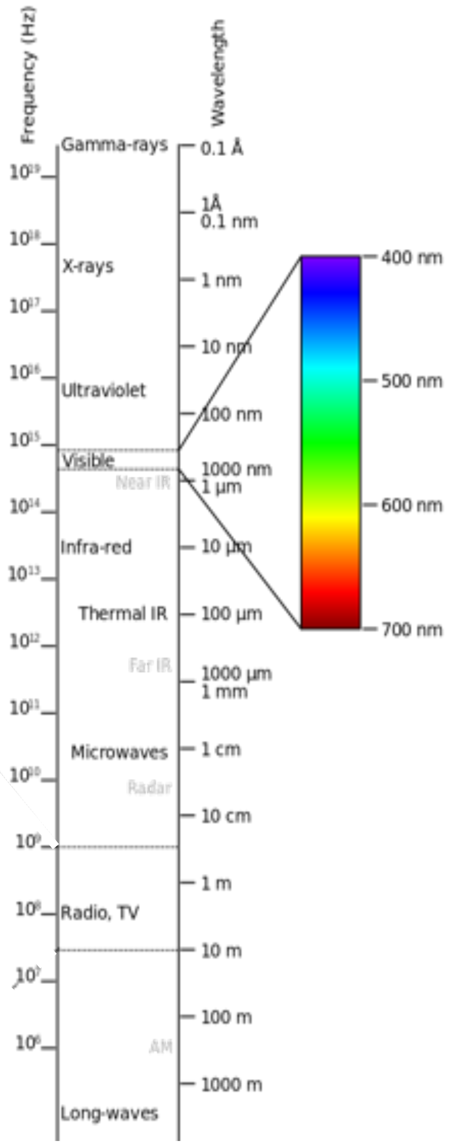

Silicon Solar cells

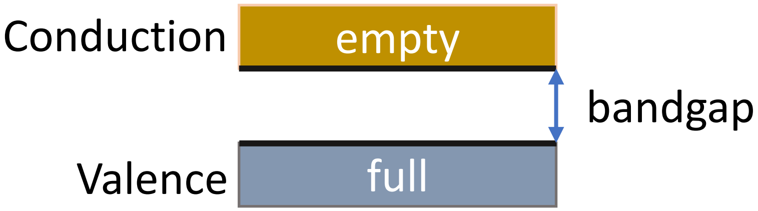

Conduction

empty

bandgap

Valence

full

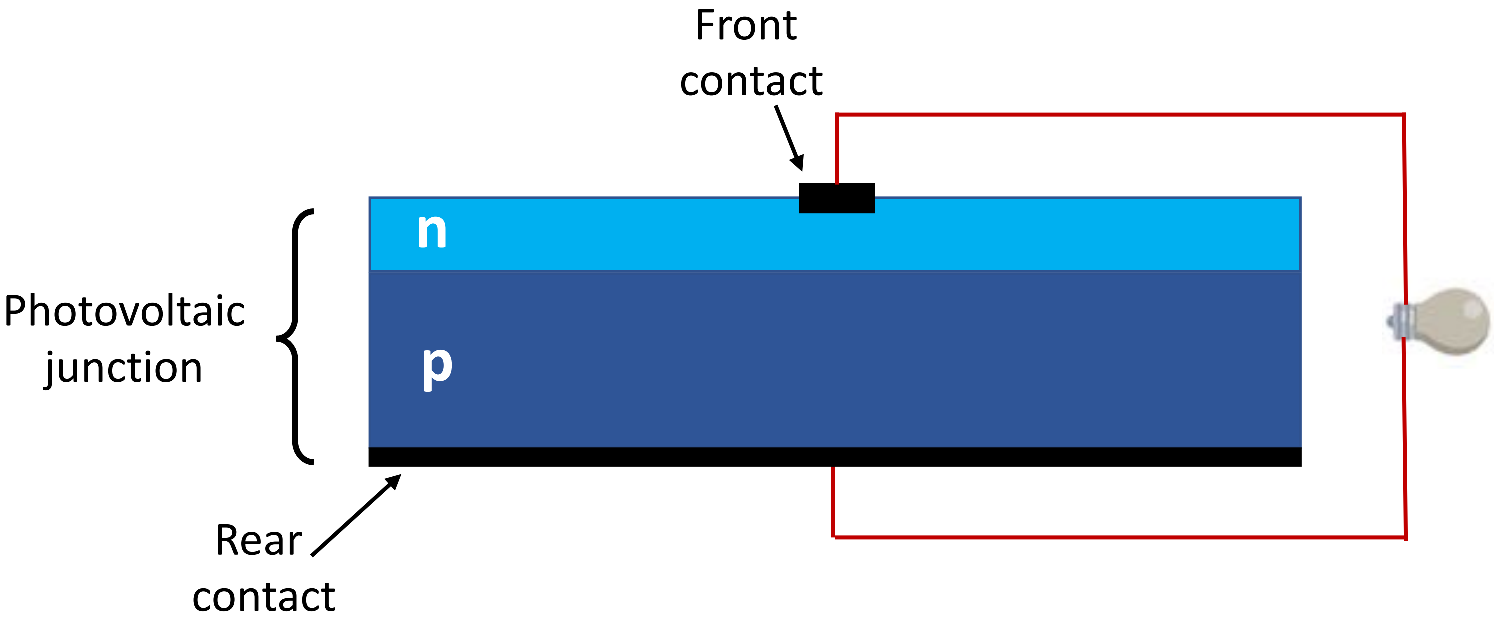

Front contact

n

p

Photovoltaic junction

Rear contact

Silicon Solar cells

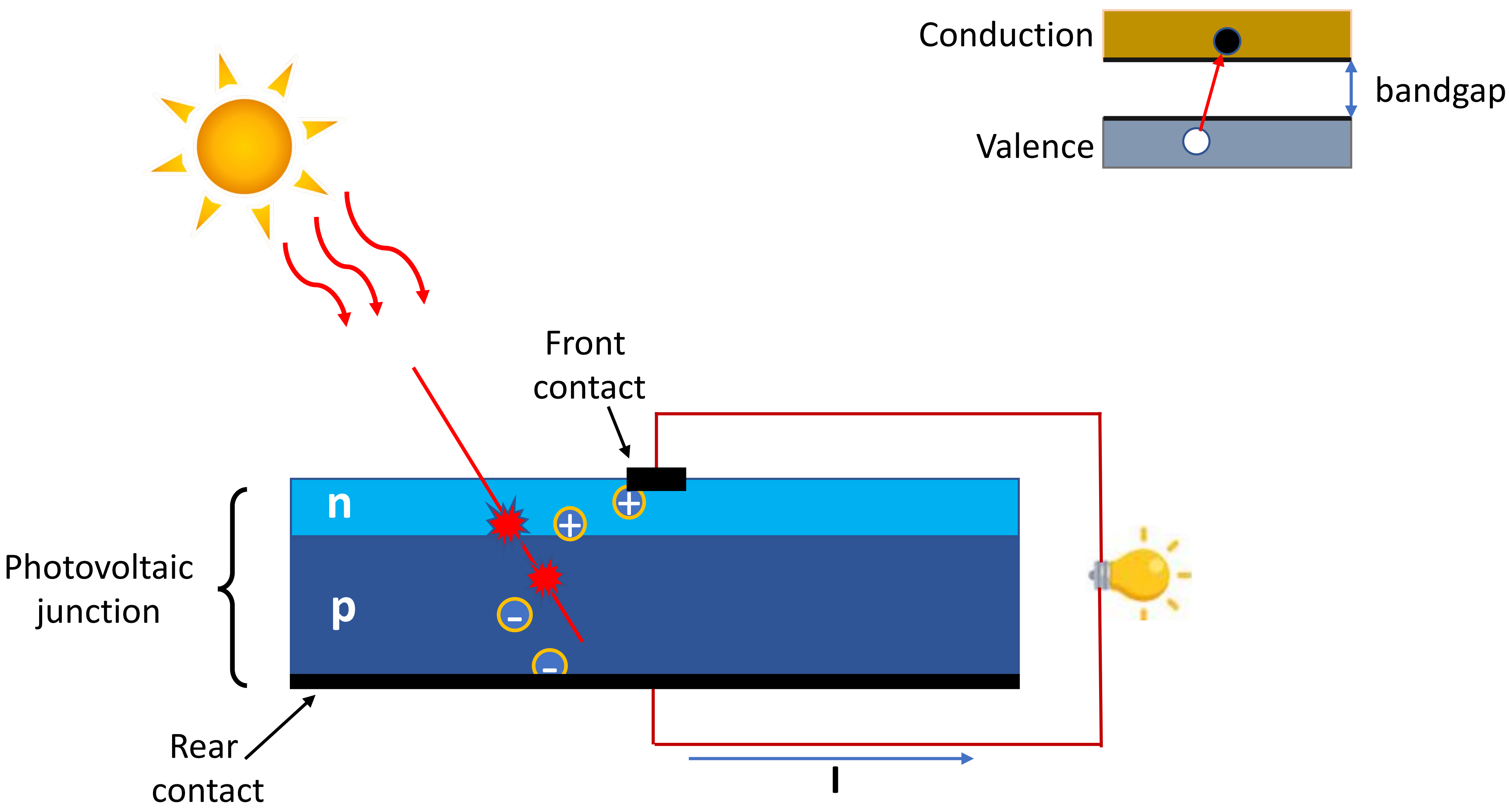

Limiting factors to conversion efficiency

Reflections

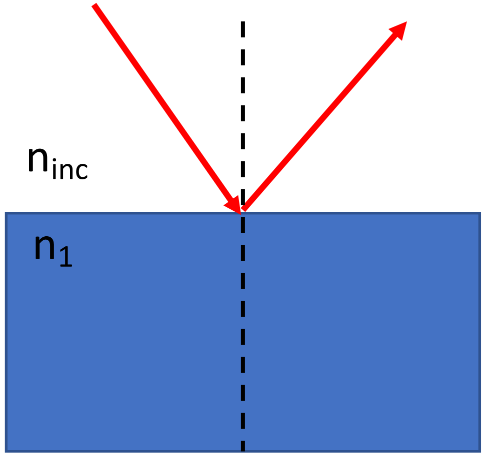

Reflections (Fresnel's equation):

$$dN_R(\lambda) = dN_0(\lambda)\left(\frac{n_1(\lambda) - n_{inc}(\lambda)}{n_1(\lambda) + n_{inc}(\lambda)}\right)^2$$

***Reflection losses**:* "an untreated surface of plane silicon reflects 36% of the normal incident sunlight for the AM 1.5 spectrum".

Peters et al., PHOTONIC CONCEPTS FOR SOLAR CELLS, Physics of Nanostructured Solar Cells (2010).

Absorption thickness

Refractive index: $n(\lambda) - ik(\lambda)$

Absorption coefficient: $\alpha = \frac{4\pi k}{\lambda}$

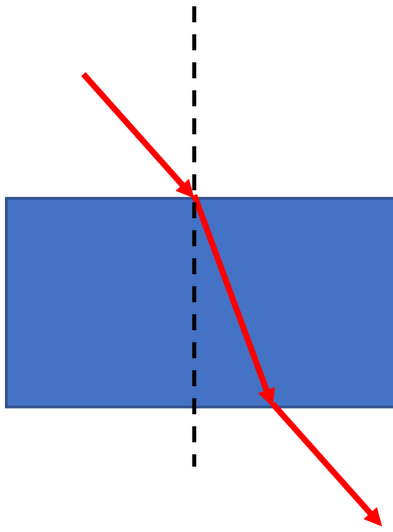

Transmission depth (Lambert-Beer's equation):

$$dN_t(\lambda) = dN_{0,i}(\lambda) \cdot \exp(-\alpha(\lambda) \cdot l)$$

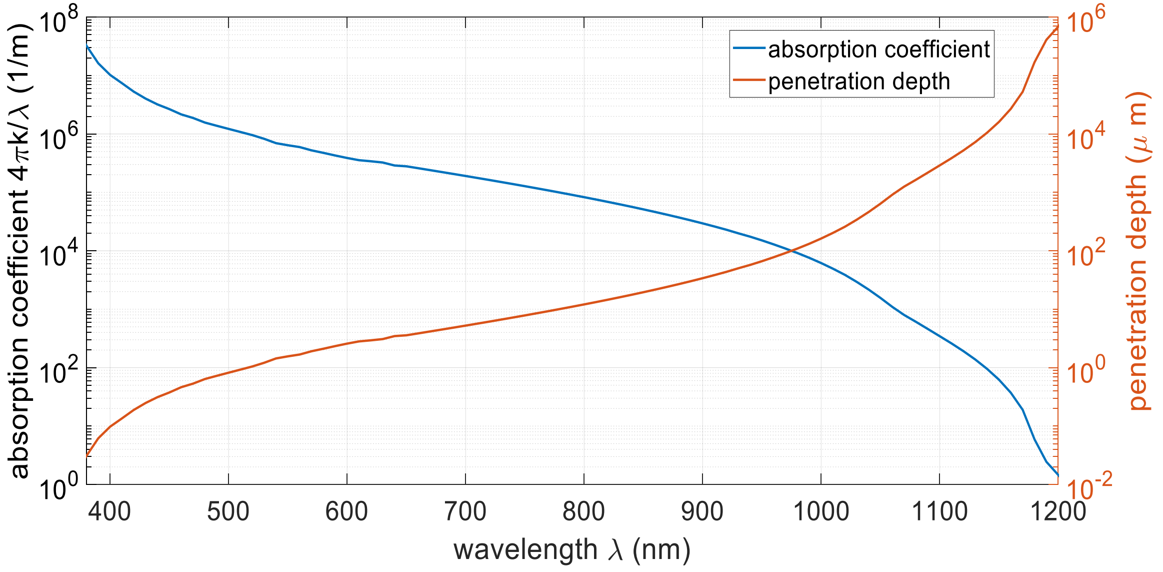

Data from https://refractiveindex.info/?shelf=main&book=Si&page=Schinke

Recombination electrons/holes

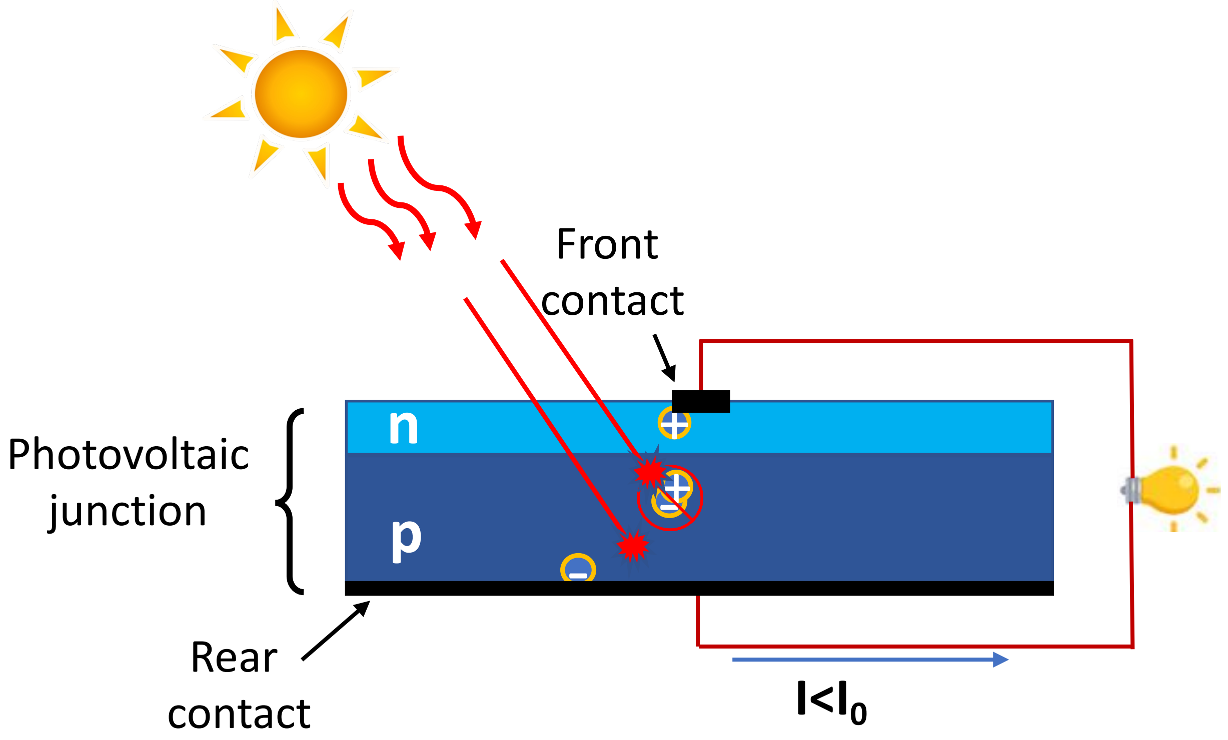

- Auger
- Trapped assisted recombination

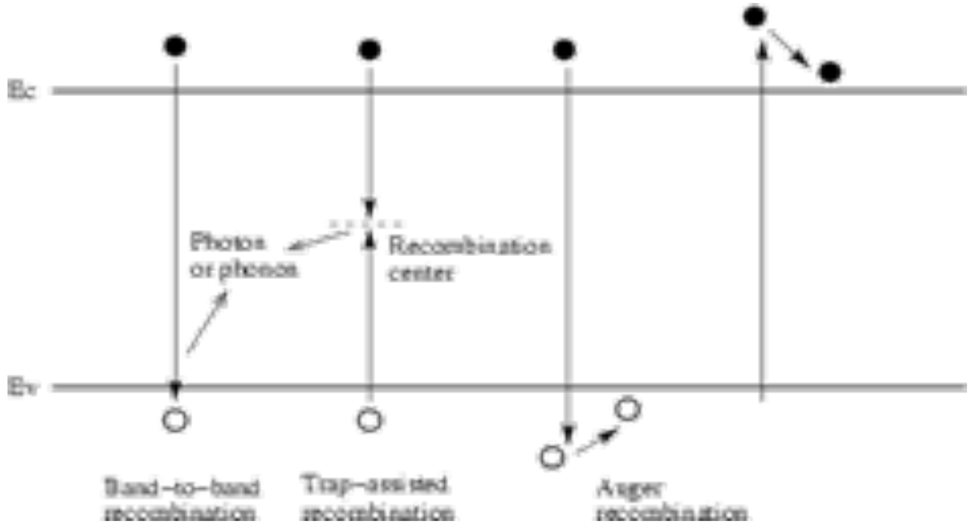

The probability of ***Recombination*** increases with the thickness of the junction

Solutions to cope with common limitations

Anti reflection

Sol. Fresnel's eq. → $n_k = \sqrt{n_1 \cdot n_s}$

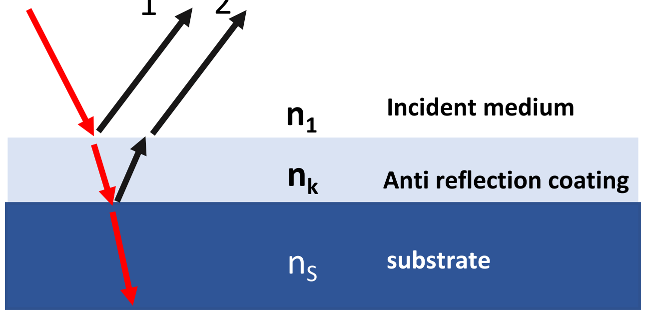

Recombination: Si thickness

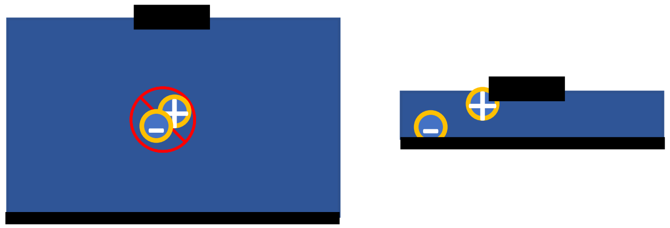

Increase light absorption:

Reflecting mirror

Surface texture

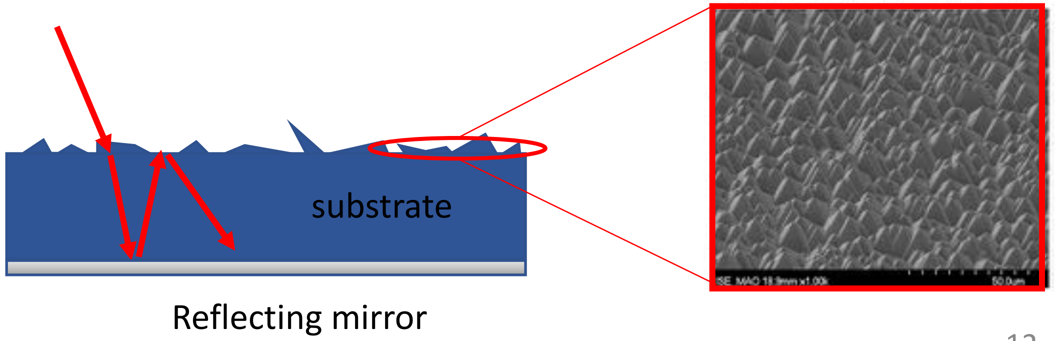

Light trapping in conventional designs

Lambertian surface

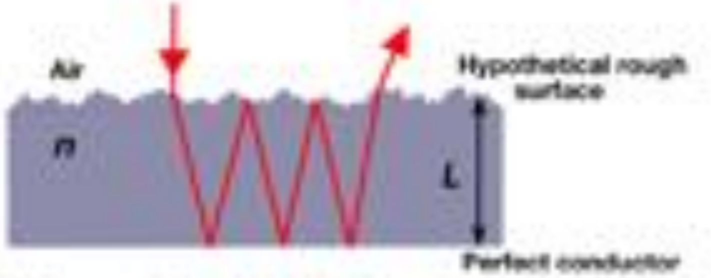

FIG. 1. Geometry used to model statistical ray-trapping in a slab with thickness L and refractive index n, placed on a perfect reflector. The randomly rough top surface is assumed to perfectly transmit all incoming rays into the slab and assumed to provide perfect total internal reflection for rays within the slab incident at an angle greater than the critical angle.

$$critical\ angle\ \theta_c = \sin^{-1}(1\backslash\mathrm{n})$$

'The top surface randomly redirects both the externally incident rays and total internally reflected rays within the slab at an angle ϑ with respect to the surface normal, according to a distribution function f (ϑ).'

- **Probability of escape**

$$\mathrm{p}=\int_0^{2\pi} d\varphi \int_0^{\theta_c} \sin\theta \left(\frac{1}{\pi}\cos\theta\right) d\theta = \frac{1}{n}$$

- **Probability of escape at the q$^{\text{th}}$ reflection**

$$G(q) = p(1-p)^{q-1} \longrightarrow \langle q\rangle = n^2$$

- **Average path length**

$$L_{avg}=\int_0^{2\pi} d\varphi \int_0^{\theta_c} \sin\theta \left(\frac{1}{\pi}\cos\theta\right) \frac{2L}{\cos\theta} d\theta = 4L$$

$$\Big\Downarrow$$

$$\boxed{L_{trap} = 4\mathrm{L}n^2}$$

*Sayak Bhattacharya *and* Sajeev John, "Photonic crystal light trapping: Beyond 30% conversion efficiency for silicon photovoltaics" , APL Photonics 5, 020902 (2020) https://doi.org/10.1063/1.5128664

Theoretical limits of solar cells efficiency: Lambertian limit

The Lambertian model establishes a superior limit to the conversion efficiency of Si solar cells

Absorption coefficient $A_{Lam}(\lambda) = \frac{\alpha(\lambda)}{\alpha(\lambda) + \frac{1}{L_{trap}(\lambda)}}$ with $\alpha(\lambda) = \frac{4\pi k}{\lambda}$

Maximum achievable photo current density $MAPD = \int_{\lambda=300nm}^{\lambda_{max}} \frac{e\lambda}{hc} I(\lambda)\, \mathrm{A}(\lambda)\, \mathrm{d}\,\lambda$

Theoretical limits of solar cells efficiency: thermodynamical limit

The Shockley Queisser Efficiency Limit

Single junction solar cells

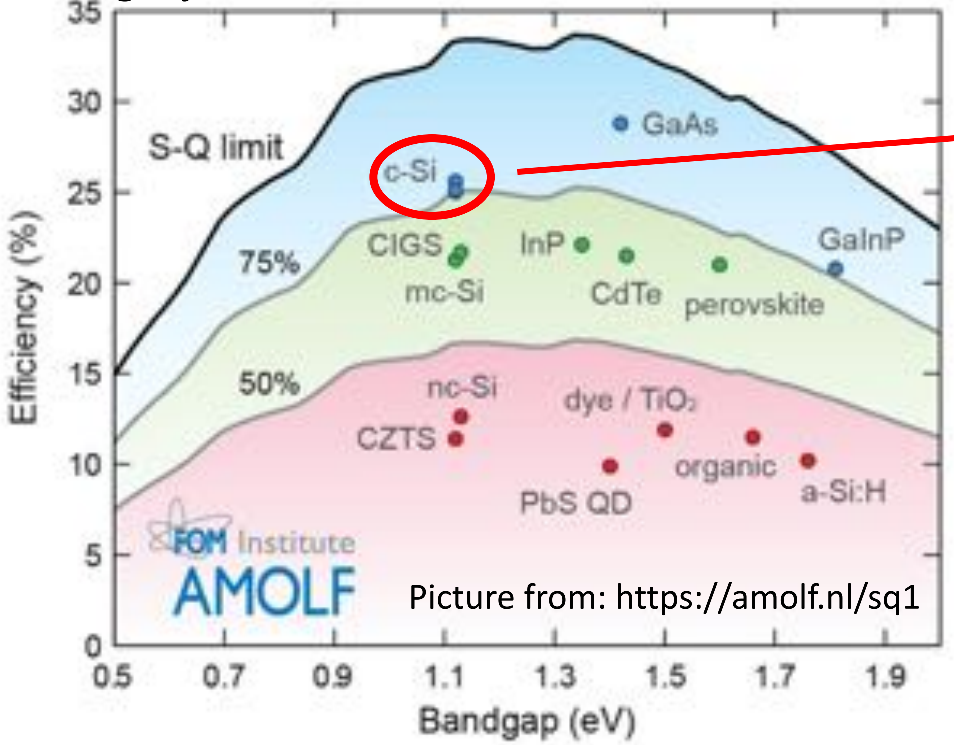

Picture from: https://amolf.nl/sq1

Single junction silicon solar cells:

- Current world-record: **26.7%** (165 μm thick)*
- Ideal Lambertian cell: **29.1%** (165 μm thick)
- Theoretical limit: 32.33% (165 μm thick)

* Yoshikawa, K., Kawasaki, H., Yoshida, W. *et al.* Silicon heterojunction solar cell with interdigitated back contacts for a photoconversion efficiency over 26%. *Nat Energy* **2,** 17032 (2017). https://doi.org/10.1038/nenergy.2017.32

Photonic crystals

Photonic crystals: definition

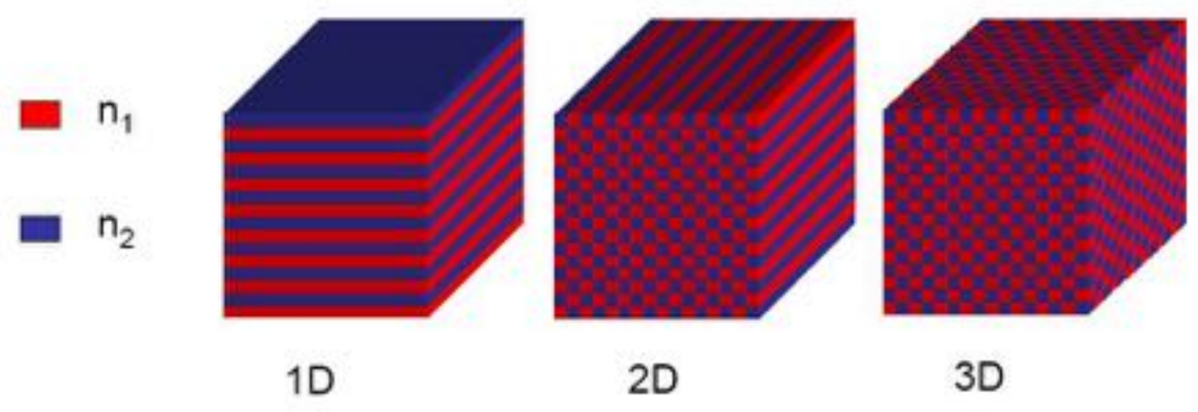

- Materials with a spatially and periodically varied refractive index are called photonic crystals.
- the period length of photonic crystals is related to the wavelength of the light being considered.
- In the field of optics, typical lattice constants are in the range of several 100nm (three orders of magnitude larger than normal crystals)

Photonic crystals analogy with semi-conductors:

$$\nabla \times \frac{1}{\varepsilon(r)} \nabla \times \vec{H}_\omega(r) = \frac{\omega^2}{c^2} \cdot \vec{H}_\omega(r), \quad \varepsilon(r+R) = \varepsilon(r) \quad \Longleftrightarrow \quad \left(\frac{\hat{p}^2}{2m} + V(r) \right) \Psi_k(r) = E \cdot \Psi_k(r), \quad V(r+R) = V(r)$$

Bandgap

A band gap is an energy range in which propagation of light within the photonic crystal is allowed.

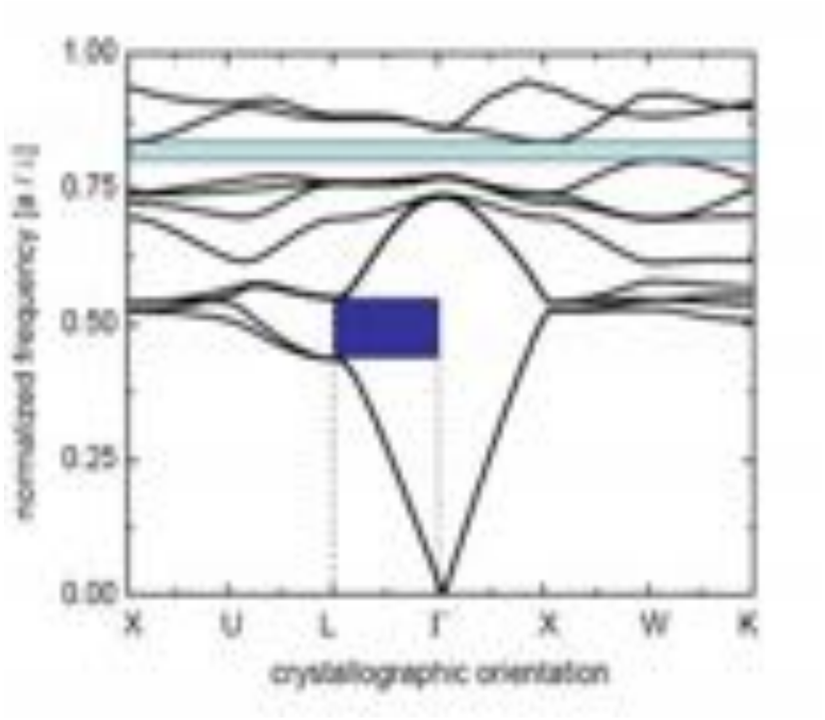

Main characteristics:

- 1D crystals are employed as mirrors

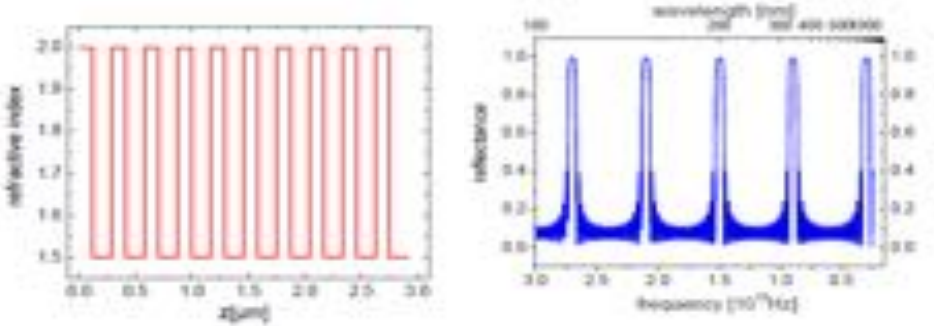

- 2D crystals: grating structures are especially useful for photon management because of diffractive effects

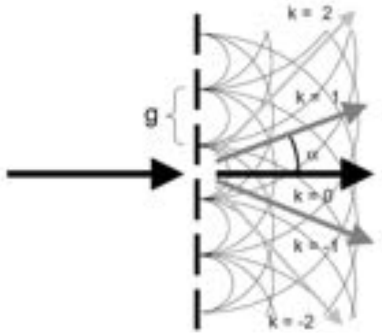

- 3D crystals: combine spectral and angular selectivity and diffractive effects

Photonic crystals (PhC) in solar cells

Wave-interference based light-trapping in photonic crystals*

*Sayak Bhattacharya *and* Sajeev John, "Photonic crystal light trapping: Beyond 30% conversion efficiency for silicon photovoltaics" , APL Photonics 5, 020902 (2020) https://doi.org/10.1063/1.5128664

Light trapping structures

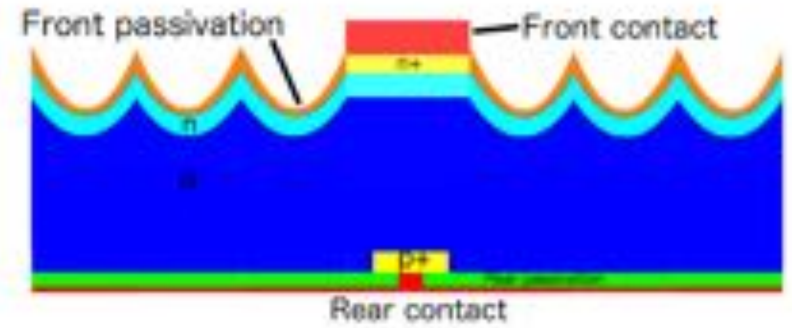

Parabolic-pore texture

Bhattacharya and S. John, "Designing high-efficiency thin silicon solar cells using parabolic-pore photonic crystals," Phys. Rev. Appl. 9, 044009 (2018).

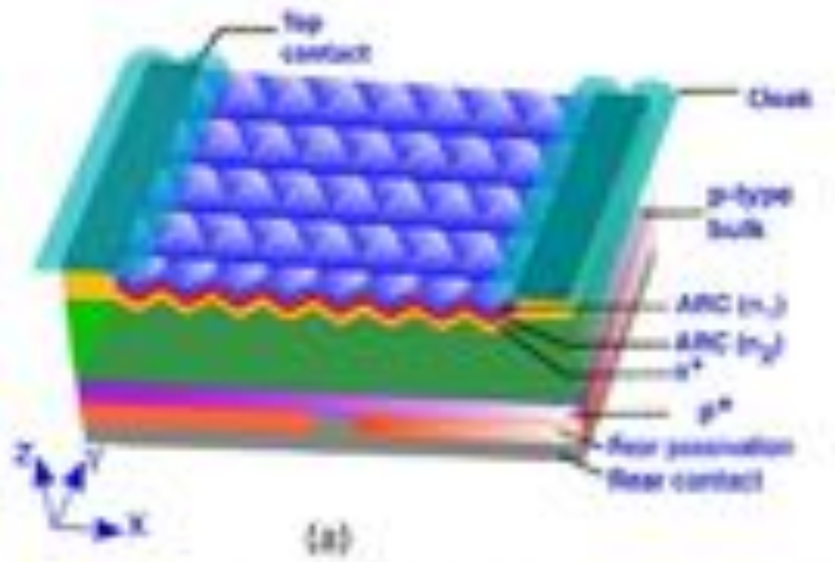

Inverted pyramid texture

*Sayak Bhattacharya *and* Sajeev John, "Photonic crystal light trapping: Beyond 30% conversion efficiency for silicon photovoltaics" , APL Photonics 5, 020902 (2020) https://doi.org/10.1063/1.5128664

Tepee-like texture

Kuang Ping et al., Achieving an accurate surface profile of a photonic crystal for near-unity solar absorption in a super thin-film architecture. ACS Nano 2016;10(6): 6116–24.

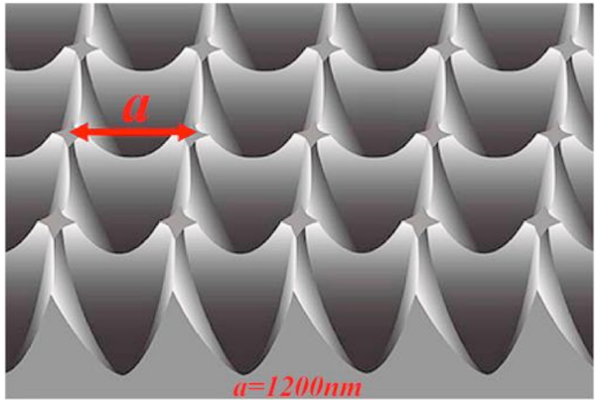

Potentials of light trapping structures

- The lattice constants of PhCs are comparable to the wavelength of light.
- Modeling of light-waves by rays would result in an inaccurate description of energy propagation.
- An accurate numerical solution of Maxwell's equations is needed in order to accurately capture the light-trapping effects.

Finite Difference Time Domain (FDTD) method

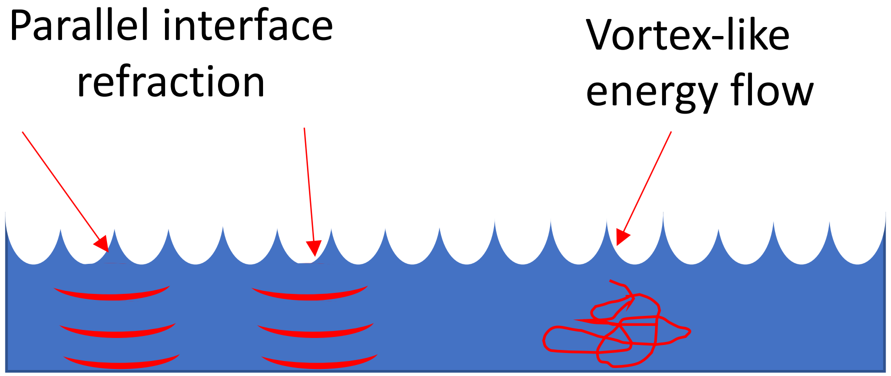
Parallel interface refraction

Vortex-like energy flow

Refraction patterns increase the time of permanence of light inside the Si cell

Optimization of lattice parameters

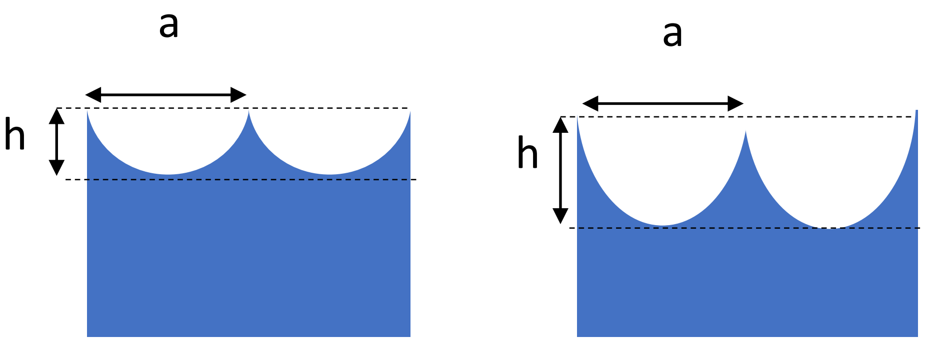

- The light absorption can be enhanced by simultaneously optimizing the pore-height (h) and lattice constant (a) of the PhC.
- The (h/a) ratio is crucial to optimizing light-trapping.

A larger (h/a) induces a more graded-index and antireflection

Vs

Deeper pores imply less light-absorbing material.

FDTD solution*

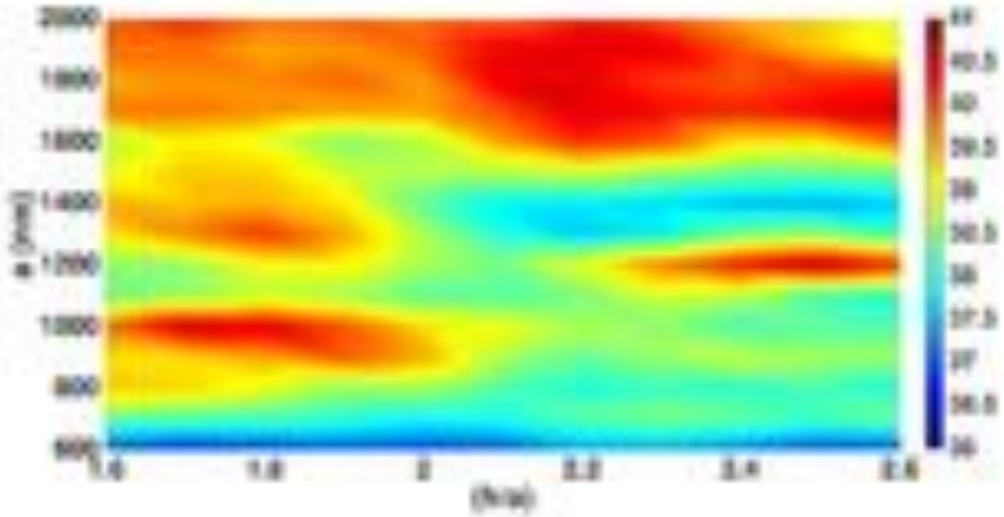

FIG. 3. MAPD optimization in 10 μm-thick vertical parabolic-pore silicon PhC with t_{SiO_2} = 100 nm, $t_{Si_3N_4}$ = 75 nm, and $t_{[illegible]}$ = 0. An optimum MAPD of 40.57 mA/cm^2 is obtained for a = 1000 nm and (h/a) = 1.8.

Breaking the symmetry 1

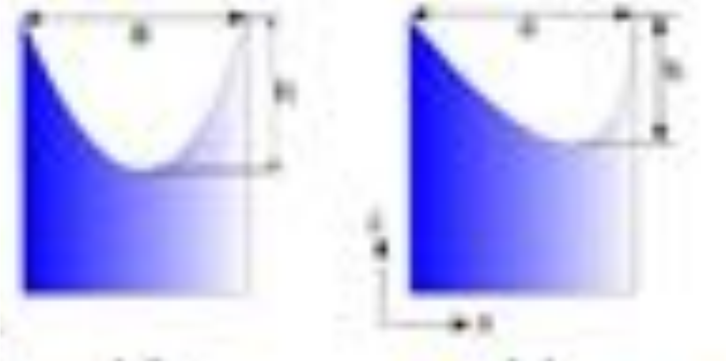

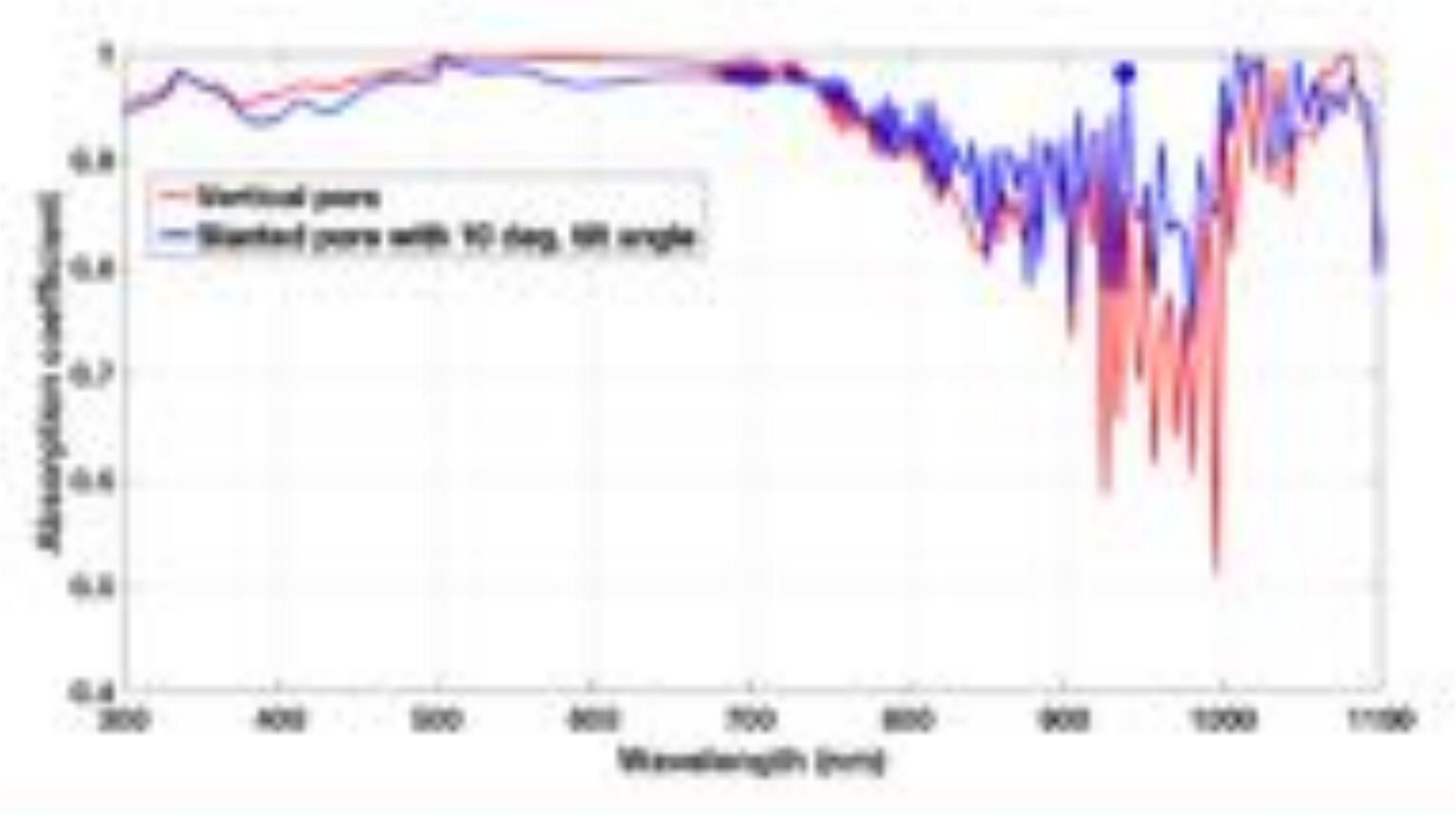

*Comparison of absorption spectra of the vertical and slanted parabolic-pore PhC structures under *y*-polarized excitation. The *x*–*y* symmetry-breaking PhC absorbs more light in 750–1000 nm wavelength range.

Breaking the symmetry 2

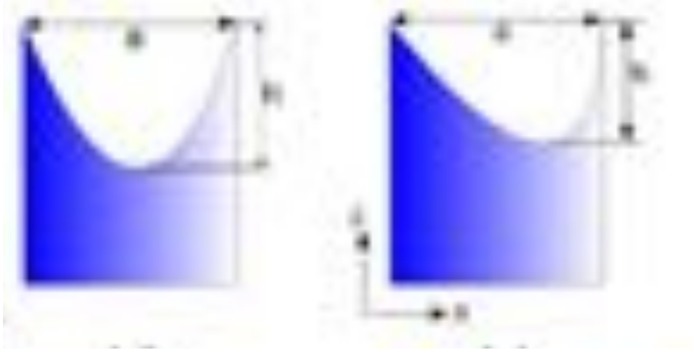

- The Poynting vectors show significant parallel-to interface power flow and prominent formation of vortices in (b) as compared to (a).
- (d) shows prominent vortices in the power flow pattern and parallel-to-interface Poynting vectors. Clearly, PIR into slow-light modes is a key mechanism for better light-trapping in the *x*–*y* symmetry-broken structure.

Plot of energy density and in-plane Poynting vector at $\boldsymbol{\lambda}$ = 940 nm*

Vertical pore

slanted pore

x-z slice

x-y slice

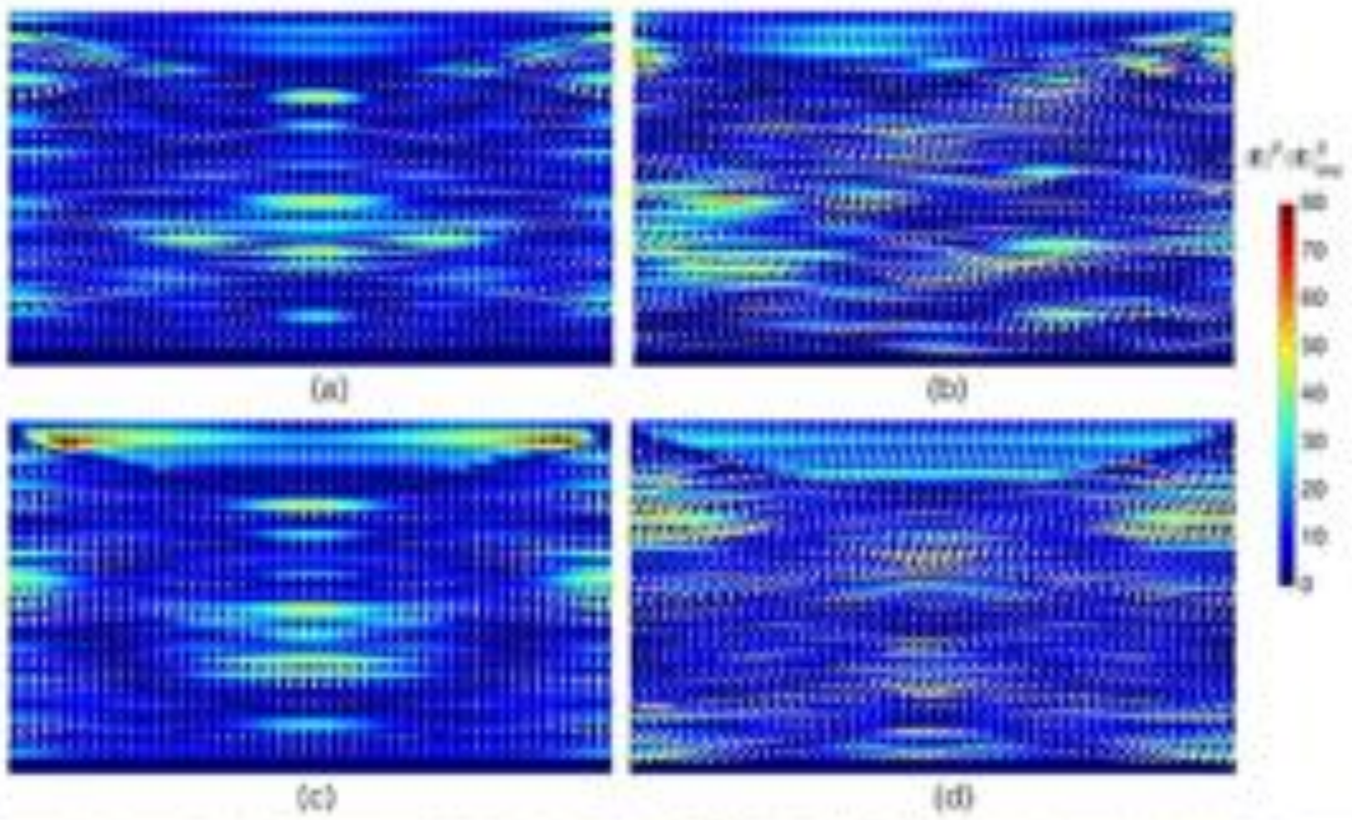

Inverted pyramid lattice

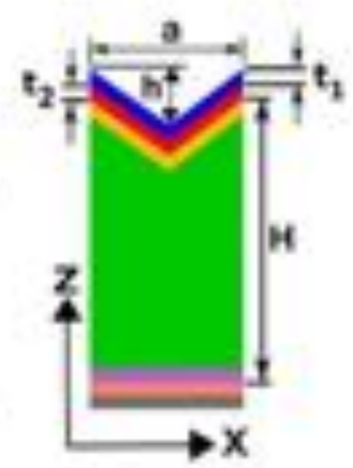

Figure 1: 2D cross section of a unit cell of the inverted micro-pyramid PhC showing FDTD design parameters. The side-wall angle of the wet-etched pyramid is 54.7° [i.e., $h/(a/2) = \tan 54.7°$].

Carrier generation rate within the unit cell of various inverted pyramid PhC solar cells:

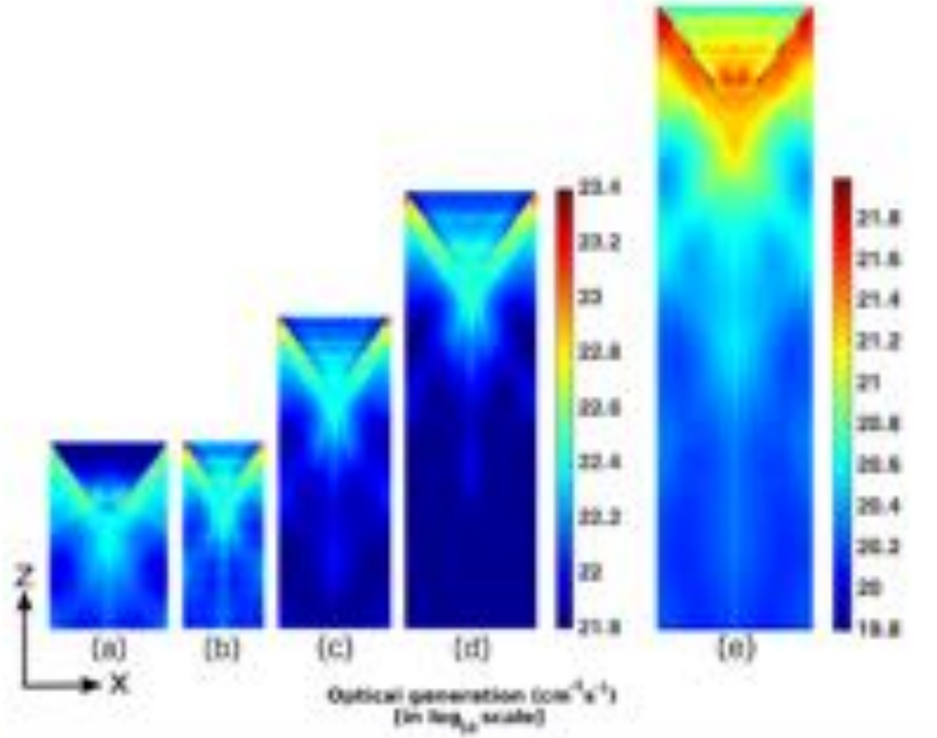

(a) $H = 3\ \mu m$, $a = 1300$ nm; (b) $H = 5\ \mu m$, $a = 1800$ nm; (c) $H = 7\ \mu m$, $a = 2100$ nm; (d) $H = 10\ \mu m$, $a = 2500$ nm; and (e) $H = 12\ \mu m$, $a = 2700$ nm.

Optimization of Inverted pyramid lattice

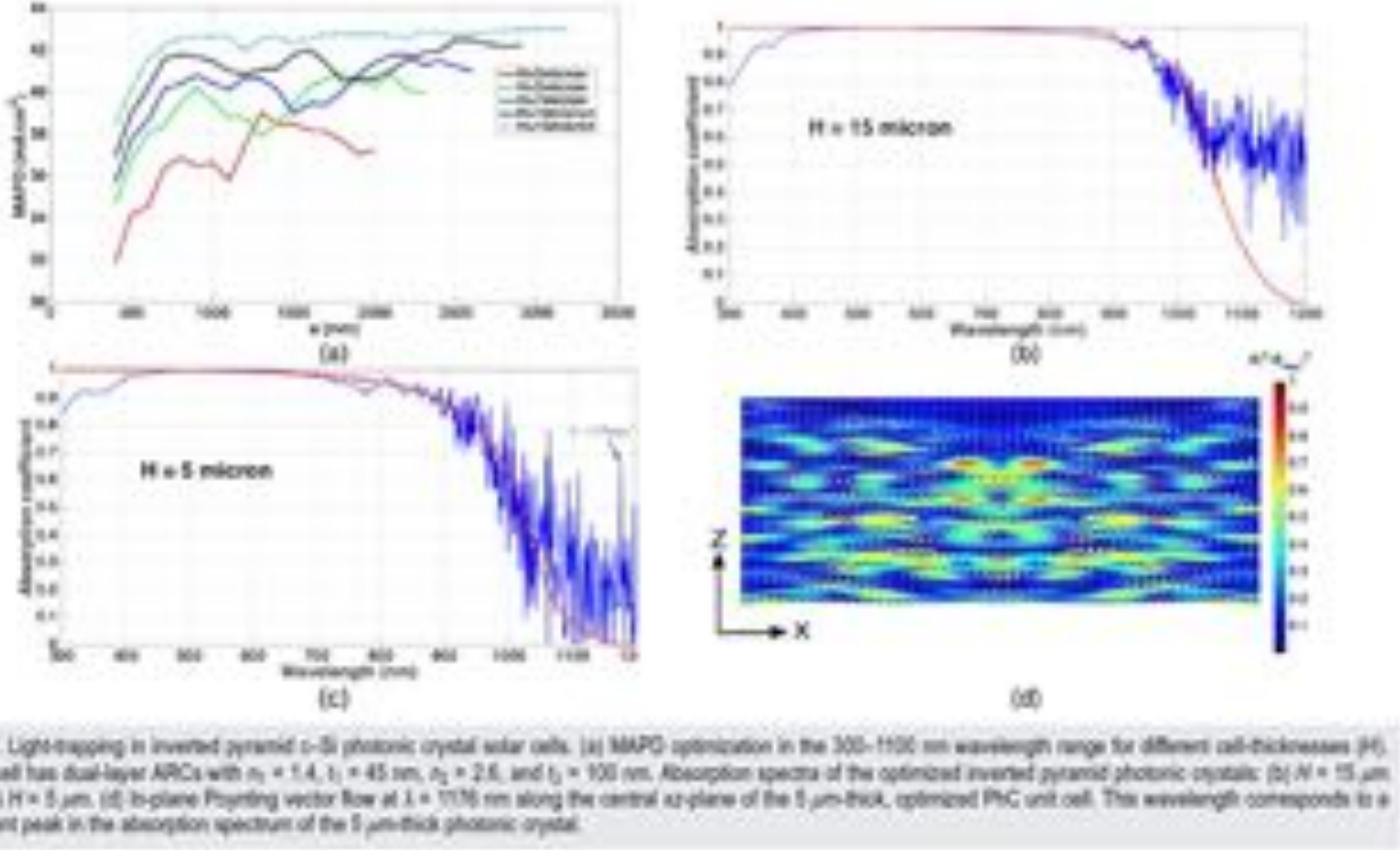

FIG. 7. Light-trapping in inverted pyramid c-Si photonic crystal solar cells. (a) MAPD optimization in the 300–1100 nm wavelength range for different cell-thicknesses (H). Each cell has dual-layer ARCs with $n_1 = 1.4$, $t_1 = 45$ nm, $n_2 = 2.6$, and $t_2 = 100$ nm. Absorption spectra of the optimized inverted pyramid photonic crystals: (b) $H = 15\ \mu m$ and (c) $H = 5\ \mu m$. (d) In-plane Poynting vector flow at $\lambda = 1176$ nm along the central xz-plane of the 5 μm-thick, optimized PhC unit cell. This wavelength corresponds to a resonant peak in the absorption spectrum of the 5 μm-thick photonic crystal.

PC crystal structures Vs Lambertian limit

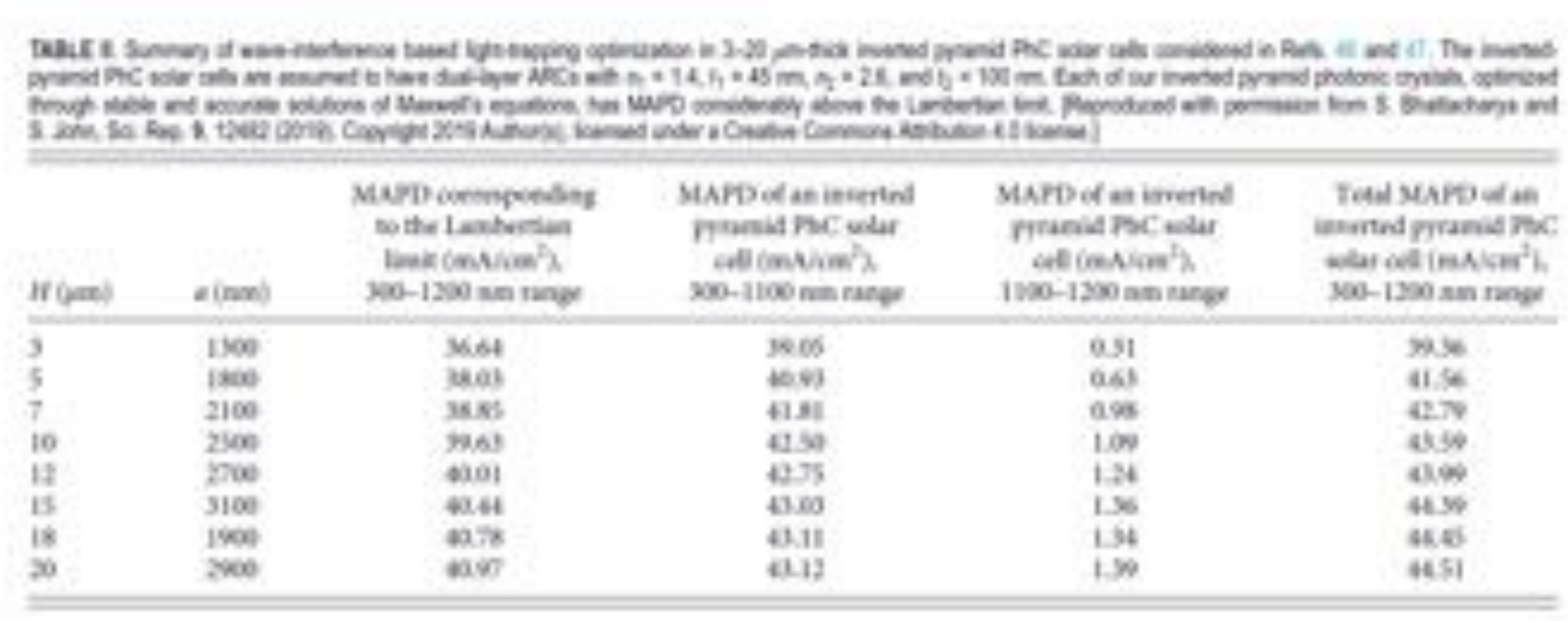

TABLE 8. Summary of wave-interference based light-trapping optimization in 3-20 μm-thick inverted pyramid PhC solar cells considered in Refs. 46 and 47. The inverted-pyramid PhC solar cells are assumed to have dual-layer ARCs with $n_1 = 1.4$, $t_1 = 45$ nm, $n_2 = 2.6$, and $t_2 = 100$ nm. Each of our inverted pyramid photonic crystals, optimized through stable and accurate solutions of Maxwell's equations, has MAPD considerably above the Lambertian limit. [Reproduced with permission from S. Bhattacharya and S. John, Sci. Rep. 9, 12482 (2019). Copyright 2019 Author(s), licensed under a Creative Commons Attribution 4.0 license.]

H (μm)	a (nm)	MAPD corresponding to the Lambertian limit (mA/cm^2), 300–1200 nm range	MAPD of an inverted pyramid PhC solar cell (mA/cm^2), 300–1100 nm range	MAPD of an inverted pyramid PhC solar cell (mA/cm^2), 1100–1200 nm range	Total MAPD of an inverted pyramid PhC solar cell (mA/cm^2), 300–1200 nm range
3	1300	36.64	39.05	0.31	39.36
5	1800	38.03	40.93	0.63	41.56
7	2100	38.85	41.81	0.98	42.79
10	2500	39.63	42.50	1.09	43.59
12	2700	40.01	42.75	1.24	43.99
15	3100	40.44	43.03	1.36	44.39
18	1900	40.78	43.11	1.34	44.45
20	2900	40.97	43.12	1.39	44.51

Conclusions

- The wave-interference based solar absorption allows reducing the thickness of solar cells
- 10–15 μm-thick inverted micro-pyramid photonic surpass the Lambertian limit for solar absorption over the 300–1200 nm wavelength range.
- The efficiency of 15 μm-thick PhC cell is significantly higher than the best 165-μm thick-silicon cells: **31%** Vs 26.7% (Kaneka).
- The efficiency PhC-based cell is even higher than the best direct bandgap GaAs cell with 29.1% efficiency.
- Such high-efficiency silicon solar cells may also be thin and flexible: suitable for integration into buildings and other power-consuming devices

Other applications

Back-reflectors

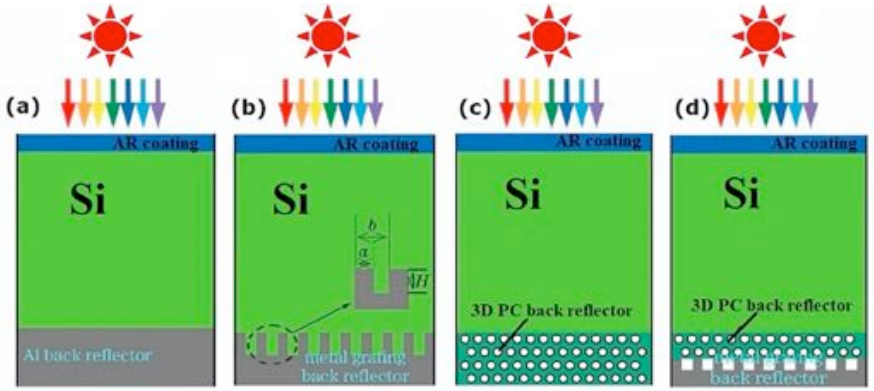

He Xiaojin, Liu Min, Zhang Yaoyao, Liu Xueqin. Study on improving light absorption of Si thin-film solar cells with metal grating and photonic crystals back reflectors. Laser Optron Prog (2016)

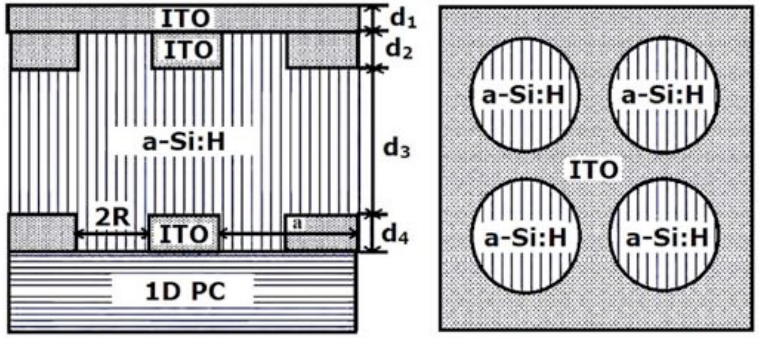

(a) Schematic of solar cell

(b) Top view of 2D PC

Selective light filter

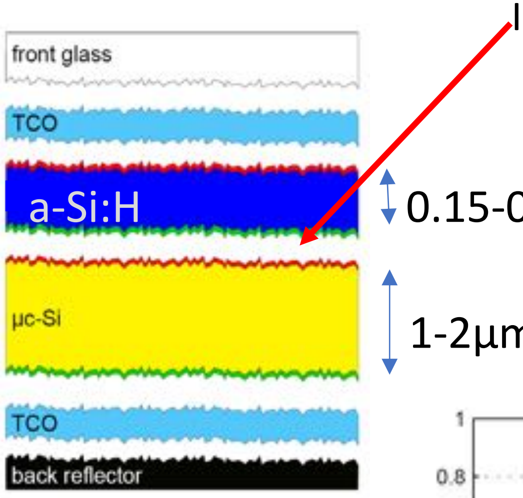

Inverted opal PhC

0.15-0.2µm

1-2µm

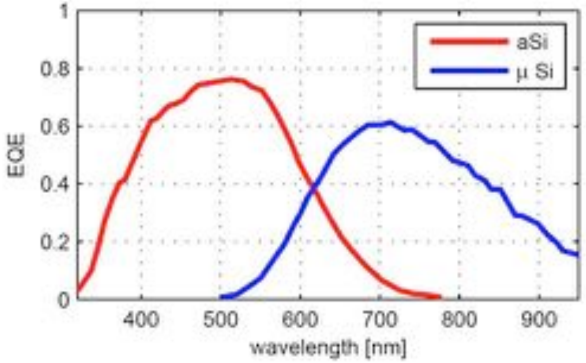

WU Zhen-hua, Si-min LI, Wen-tao ZHANG, GAO Feng-yan. Back reflector of solar cells consisting of one-dimensional photonic crystal and double-layered two-dimensional photonic crystal. Acta photonica, 45(2), (2016)